Non-linear MHD modeling of internal kink mode in tokamaks

F.D. Halpern, H. Lütjens, J.-F. Luciani

Centre de Physique Théorique, CNRS, École Polytechnique, 91120 Palaiseau, France

Sawtooth oscillations were first observed in the 1970s in small, ohmically-heated experiments [1, 2]. They are characterized by a sudden, periodic crash of the plasma central temperature caused by a reconnecting internal kink mode with helicity $q = m/n = 1$. In the present work, the two-fluid MHD code XTOR-2F [3] is used to investigate the dynamics of sawtooth cycling in tokamaks. In particular, following a study on the dynamics of the internal kink in resistive MHD [4], we concentrate on the effects of ion and electorn diamagnetic drifts on kink oscillations. The present work attempts to describe the ramp phase of sawtooth oscillations, and how the diamagnetic drift terms affect the regimes where sawtoothing can occur.

The physical model implemented in the XTOR-2F code is fully toroidal and non-linear; it include anisotropic thermal transport, resistivity, viscosity, and diamagnetic drifts. The equations used the present study are

$$\rho\partial_t\mathbf{v} = -\rho\left(\mathbf{v}\cdot\nabla\right)\mathbf{v} - \rho\left(\mathbf{v}_\mathbf{i}^*\cdot\nabla\right)\mathbf{v}_\perp + \mathbf{J}\times\mathbf{B} - \nabla p + \nabla^2\mathbf{v}, \quad (1)$$

$$\partial_t\mathbf{B} = \nabla\times\left(\mathbf{v}\times\mathbf{B}\right) + \alpha\nabla\times\nabla_\parallel p_e/\rho - \nabla\times\eta\mathbf{J}, \quad (2)$$

$$\partial_t p = \Gamma p\nabla\cdot\mathbf{v} - \mathbf{v}\cdot\nabla p - \alpha\Gamma\frac{p}{\rho}\nabla p_i\cdot\nabla\times\mathbf{B}/B^2 + \nabla\cdot\chi_\perp\nabla(p - p_{t=0}) + \nabla\cdot\left[\mathbf{B}\left(\chi_\parallel/B^2\left(\mathbf{B}\cdot\nabla\right)p\right)\right], \quad (3)$$

$$\partial_t\rho = -\rho\nabla\cdot\mathbf{v} - \mathbf{v}\cdot\nabla\rho - \alpha\nabla p_i\cdot\nabla\times\mathbf{B}/B^2 + \nabla\cdot D_\perp\nabla(\rho - \rho_{t=0}). \quad (4)$$

In the above equations, $\nu = 5.0\times10^{-6}$ is the viscosity, $\eta = 1.0\times10^{-6}(p/p_{x=0})^{-3/2}$ is the resistivity, $\chi_\perp = 3.0\times10^{-5}(p/p_{x=0})^{-3/2}$ is the perpendicular thermal diffusivity, $\chi_\parallel = 100$ is the parallel heat diffusivity, $D_\perp = \chi_\perp/10$ is the particle diffusivity, and Γ is the ratio of specific heats. The ion diamagnetic velocity is given by $\mathbf{v}_i^* = \alpha\mathbf{B}\times\nabla p_i/(\rho B^2)$; while $\alpha = (\omega_{ci}\tau_a)^{-1}$ is a scaling constant for the diamagnetic drifts ($\omega_{ci} = ZeB_u/m_i$ is the ion cyclotron frequency, $\tau_A = (\mu_0\rho_{x=0})^{1/2}a/B_u$ is the Alfvén time, $B_u = B_0 a/R$ is the unit magnetic field, Z is the charge number, a is the minor plasma radius, and R is the major radius). Equal ion and electron pressure, $p_e = p_i = p/2$ is assumed. The diffusive terms in Eqs. 3 and 4 restore the pressure and density profiles within their characteristic diffusion time.

In internal XTOR units, the Alfén time $\tau_a = 1$, while the minor radius $a = 1$. This choice of units gives the central Lundquist number $S = 1/\eta_{x=0}$; the characteristic resistive time $\tau_\eta = 1/\eta$; and the resistive energy diffusion time $\tau_{\chi_\perp} = 1/\chi_\perp$. The relevant timescales of the plasma

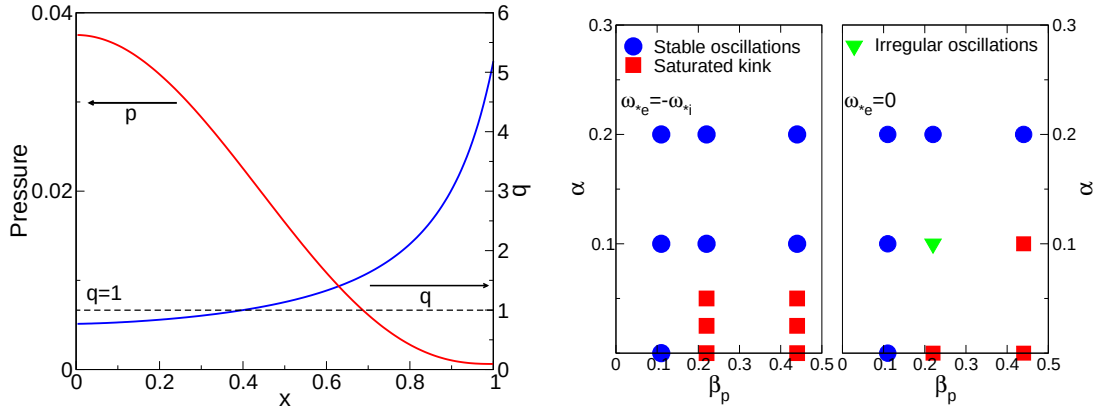

Figure 1: Left panel: Pressure (red) and magnetic q (blue) equilibrium profiles used in the study. Right panel: Oscillation regimes as a function of α and β_p, with both diamagnetic drifts (left) and with only the ion diamagnetic drift (right)

dynamics are given by the resistivity η, which affects the growth rate of the internal kink and the relaxation of the q profile after each crash; and $\chi_\perp$, which affects the build-up time of the pressure through the source term in Eq. 3. Simulations are carried out using $\tau_\eta/\tau_{\chi_\perp} = \chi_\perp/\eta = 30$, while in tokamak experiments $\chi_\perp/\eta \approx 100$. The results shown correspond to the non-linear quasi-steady state.

Simulations are carried out in plasmas that approximate the conditions found in ohmically heated low performance tokamak discharges. The starting equilibrium pressure and current profiles, shown in Fig. 1, are computed using the CHEASE code [5]. The equilibrium is circular, with aspect ratio $A = R/a = 2.7$. The q profile is almost parabolic, with $q_0 = 0.77$, $q_{edge} = 5.2$, and magnetic shear $\hat{s}_{q=1} = 0.4$ at the $q = 1$ surface ($\hat{s} = (r/q)(dq/dr)$). Scans in poloidal beta, $\beta_p = 2\mu_0 p/B_\theta^2$, are carried out by rescaling the pressure. The threshold for the ideal MHD kink for this current profile is $\beta_p = 0.33$. We remark that the final steady-state of the oscillating system depends on the current and pressure drives rather than on the initial equilibrium conditions.

Non-linear simulations are carried out at different values of β_p, with and without diamagnetic rotation effects. The non-linear simulations yield different internal kink regimes, as shown on the right panel of Fig. 1. Note that simulations carried out with $\alpha = 0$ yield results equivalent to previous studies [4]. A regime characterized by periodic, non-decaying oscillations (blue circles in Fig. 1) is recovered at low β_p, or high α. First, during the ramp-up phase, the pressure profile peaks in the center due to the source term. The unstable kink mode grows, slowly pushing the core pressure (which spirals outwards due to the diamagnetic drifts) against the $q = 1$ surface, and a reconnection layer appears. Then, the pressure is evacuated outwards, through the resonant surface. The core pressure becomes completely flattened inside $q = 1$, and the cycle restarts. The

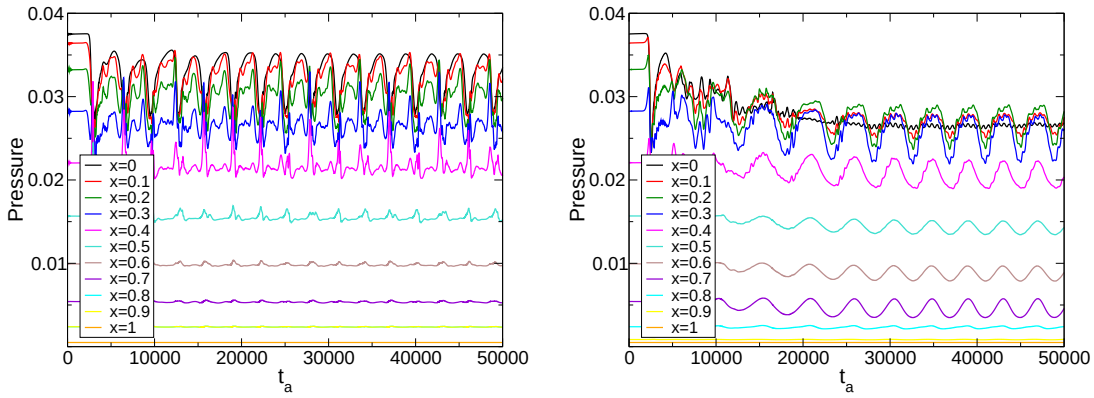

Figure 2: Presure vs. time is given at different radii for simulations in the oscillatory regime, $\beta_p = 0.22$ and $\alpha = 0.1$, (left panel) and on the saturated regime, $\beta_p = 0.22$ and $\alpha = 0.05$ (right panel). Simulations include both diamagnetic drifts, $S = 10^6$.

amplitude of the pressure oscillations is typically about 15%. The average period of the cycle is about 3000-4000τ_a, with a crash time of about 400τ_a. An example of the evolution of the central pressure in the oscillatory regime is shown on the left pannel of Fig. 2. The small oscillations observed in the pressure amplitude are due to the diamagnetic rotation of magnetic island chains at the $q = 1$ resonant surface.

At high β_p, low α (red squares in Fig. 1), the core pressure evolves into a rotating three-dimensional configuration with helicity $m/n = 1/1$. In this case, a permanent reconnection layer forms, coupled with a three-dimensional convection cell with $q \approx 1$ [6, 7]. The magnetic q profile is measured with 1% precision. The pressure and current introduced in the plasma through the source terms are continually expelled through the reconnection layer. Thus, neither the pressure nor the current accumulate inside the $q = 1$ surface. An example of the evolution of the central pressure in the saturated regime is shown on the right pannel of Fig. 2. In addition, one of the cases results in an unclear pattern of periodic kinks of irregular periods, amplitudes, and large island chains (of varying amplitude) at the $q = 1$ surface rotating around the plasma.

A simulation with $\beta_p = 0.22$, with both ion and electron diamagnetic rotations, is carried out with $S = 10^7$, but changing the transport coefficients in order to keep $\tau_\eta/\tau_{\chi_\perp} = 30$, and other ratios of characteristic times the same as before. The length of the cycle compared to the crash time is increased considerably respect to the case with $S = 10^6$. The simulation yields a period of about 25000τ_a, and consequently the ramp dynamics can be examined in detail. Part of the ramp is quiescent, as shown in the pressure evolution plot on the left panel of Fig. 3. It is found that, after a ramp similar to the stable oscillation regimes, the precursor growth is stabilized. Suddenly, the kinetic energy of the modes, shown on the right panel of Fig. 3,

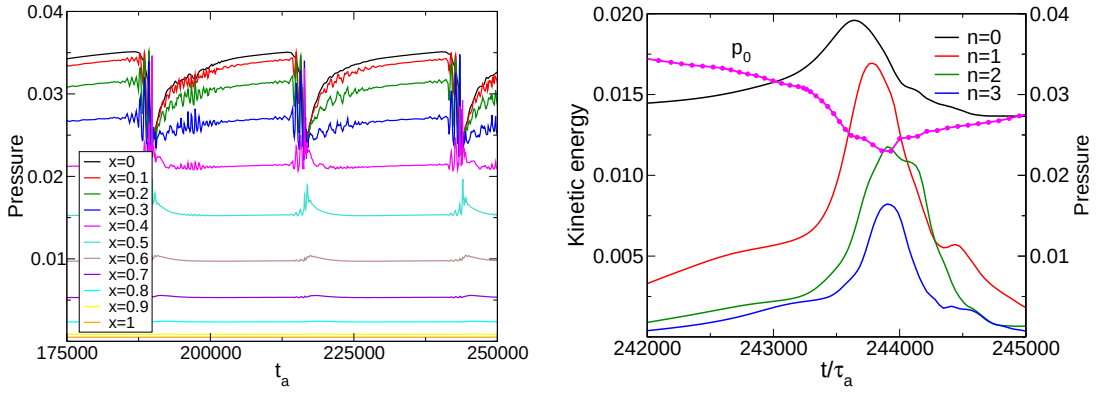

Figure 3: Left: Presure vs. time in simulation carried out with $S = 10^7$, $\beta_p = 0.22$, and $\alpha = 0.1$. Right: kinetic energy of $n = 0, 1, 2, 3$ modes and p_0 during one crash on the left panel.

triples in $500\tau_a$. This behavior is consistent with previous reports of acceleration of the growth rate [8, 9]. We note that the pressure crash takes place in two stages, that correspond, first, to the slow spiraling-out of the pressure during the precursor stage, and then to the fast evacuation due to the accelerated mode growth. Possibly, the crash can be interpreted as a transition from a quasi-saturated mode to a rapidly growing mode driven by the loss of the electron diamagnetic stabilization.

References

[1] S. von Goeler, W. Stodiek, and N. Sauthoff, Phys. Rev. Letters **33**(20), 1201 (1974).

[2] B. B. Kadomtsev, Soviet Journal of Plasma Physics **1**, 389 (1975).

[3] H. Lütjens, J. Luciani, D. Leblond, F. Halpern, and P. Maget, Plasma Physics and Controlled Fusion **51**(12), 124038 (2009).

[4] D. Leblond, H. Lütjens, and J.-F. Luciani, in *36th EPS Conference on Plasma Physics*, European Physical Society, Sofia (2009), vol. 33E, pp. P–1.127.

[5] H. Lütjens, A. Bondeson, and O. Sauter, Comp. Phys. Comm. **97**(3), 219 (1996).

[6] R. E. Denton, J. F. Drake, and R. G. Kleva, Physics of Fluids **30**(5), 1448 (1987).

[7] F. L. Waelbroeck and R. D. Hazeltine, Phys. Fluids **31**(5), 1217 (1988).

[8] L. Zakharov, B. Rogers, and S. Migliuolo, Phys. Fluids B **5**(7), 2498 (1993).

[9] A. Y. Aydemir, Phys. Fluids B **4**(11), 3469 (1992).